

## White-Light-Emitting Edge-Functionalized Graphene Quantum Dots\*\*

Ryo Sekiya, Yuichiro Uemura, Hideki Murakami, and Takeharu Haino\*

**Abstract:** Graphene quantum dots (GQDs) have received considerable attention for their potential applications in the development of novel optoelectronic materials. In the generation of optoelectronic devices, the development of GQDs that are regulated in terms of their size and dimensions and are unoxidized at the  $sp^2$  surfaces is desired. GQDs functionalized with bulky Fréchet's dendritic wedges at the GQD periphery were synthesized. The single-layered, size-regulated structures of the dendronized GQDs were revealed by atomic force microscopy. The edge-functionalization of the GQDs led to white-light emission, which is an uncommon feature.

Carbon is a ubiquitous and important element in nature and forms millions of organic compounds in conjunction with other elements. Its various allotropes include graphite, diamond, fullerenes, and carbon nanotubes. Since the discoveries of fullerenes<sup>[1]</sup> and carbon nanotubes,<sup>[2]</sup> these two allotropes have been extensively studied for electronic applications.<sup>[3]</sup> However, obtaining chemically pure forms of fullerenes and carbon nanotubes on a gram scale is not economical, and production difficulties limit the practical development of unique carbon-based materials from these sources. By contrast, graphene,<sup>[4]</sup> a single planar sheet of  $sp^2$ -bonded carbon atoms, can be obtained from commercially available graphite. The unique chemical and physical properties of graphene make it a promising material for versatile applications in nanotechnology.<sup>[5]</sup> Among graphene derivatives, graphene quantum dots (GQDs) have received considerable attention because of their electronic and optical properties, which originate from the quantum-size effect.<sup>[6]</sup> Optical bio-imaging and photovoltaic devices can be potential applications resulting from the electronic and optical properties of GQDs.<sup>[7]</sup> These properties are influenced by the size

and dimensions of the conjugated aromatic surface. The oxidative-cutting method as reported by Hummers is typically applied to obtain GQDs and it leads to oxidation at the  $sp^2$  surfaces as well as the periphery.<sup>[8]</sup> To recover the smooth  $sp^2$  surfaces, hydrazine reduction frequently follows. However, regulating the size and dimensions of reduced GQDs remains problematic, and furthermore, oxygen-containing functionalities sometimes continue to be found on the  $sp^2$  surface. These functionalities represent major drawbacks for the production of electro- and photochemically uniform GQDs. The development of GQDs that are regulated in terms of their size and dimensions and are unoxidized at the  $sp^2$  surfaces is therefore desired.

The post-synthesis modification of GQDs is another potential strategy to regulate their chemical, electronic, and photophysical properties. Graphene surfaces and peripheries can be modified by chemical reactions. However, GQDs are mainly soluble in water and in polar solvents, thus imposing a limit on the range of chemical modifications. The post-synthesis modification of GQDs through mild chemical reactions would be welcomed as a technique for tuning the aforementioned properties. The development of a method that fulfills these requirements for GQD synthesis is a significant challenge in graphene chemistry. Herein, we report the synthesis of size-regulated GQDs through oxidative-cutting and post-synthesis functionalization with bulky Fréchet's dendritic wedges through Huisgen cycloaddition (Scheme 1).<sup>[9]</sup> Detailed structural characterizations of the periphery and the  $sp^2$  surfaces of the GQDs were also performed through spectroscopic and microscopic studies. The photochemical modulation of the GQDs was achieved through the post-synthesis modification of the GQD peripheries. Finally, functionalizing the edges of GQDs in this manner resulted in white-light emission, an uncommon effect.

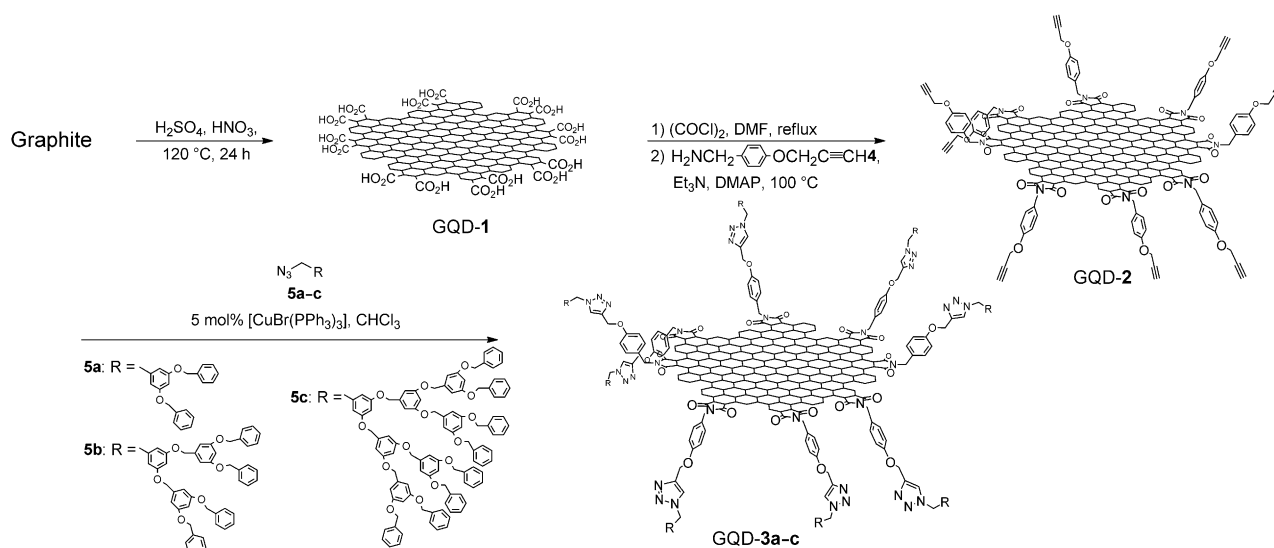
Hummers method<sup>[8]</sup> is frequently used for graphene synthesis but the potent reaction conditions do not favor a smooth  $sp^2$  surface. Among the possible exfoliation conditions of graphite that were carefully investigated, oxidative cutting of commercially available graphite by using a mixture of concentrated  $H_2SO_4$  and  $HNO_3$  (3:1, v/v) at 120 °C for 24 h gave the highest quality water-soluble GQDs (GQD-1) on a gram scale.<sup>[10]</sup> X-ray photoelectron spectroscopy (XPS) was informative for gaining structural insights into GQD-1. The XPS spectrum of GQD-1 was deconvoluted into three components with binding energies of 284.6, 286.4, and 288.5 eV, attributable to C=C, C–O, and C=O species, respectively. Graphene oxide, prepared by the traditional oxidative cutting method, shows intense C=C and C–O bands.<sup>[11]</sup> By contrast, GQD-1 predominantly displayed the C=C band. These results suggested that the  $sp^2$  graphitic

[\*] Prof. Dr. R. Sekiya, Y. Uemura, Prof. Dr. T. Haino  
Department of Chemistry, Graduate School of Science  
Hiroshima University  
1-3-1 Kagamiyama, Higashi-Hiroshima, 739-8526 (Japan)  
E-mail: haino@hiroshima-u.ac.jp

Prof. Dr. H. Murakami  
Research Institute for Nanodevice and Biosystems  
Hiroshima University  
1-4-2 Kagamiyama, Higashi-Hiroshima, 739-8530 (Japan)

[\*\*] This work was supported by Grants-in-Aid for Scientific Research (B) (No. 24350060) and Challenging Exploratory Research (No. 23655105) of JSPS, as well as Grants-in-Aid for Scientific Research on Innovative Areas, "Stimuli-responsive Chemical Species for Creation of Functional Molecules", and "New Polymeric Materials Based on Element-Blocks" (Nos. 25109529, 25102532).

Supporting information for this article is available on the WWW under <http://dx.doi.org/10.1002/anie.201311248>.



**Scheme 1.** Preparation of GQD-2 and the introduction of dendritic wedges by copper-catalyzed Huisgen cycloaddition. DMF = *N,N*-dimethylformamide, DMAP = 4-dimethylaminopyridine.

carbon network is maintained. The  $^{13}\text{C}$  NMR spectrum of GQD-1, measured in  $\text{D}_2\text{O}$ , provided supporting evidence that the  $\text{sp}^2$  graphitic carbon network for GQD-1 was not oxidized. Only  $\text{sp}^2$  carbon and carbonyl carbon resonances were observed, with no signals present in the aliphatic region. By contrast, solid-state  $^{13}\text{C}$  MAS NMR spectra of graphene oxides prepared by Hummers method indicated oxidized  $\text{sp}^3$  carbon atoms with resonances at  $\delta = 59.1$  and  $69.0$  ppm.<sup>[12]</sup> Accordingly, no  $\text{sp}^3$ -hybridized carbon atoms bearing epoxide or alcohol functionalities were formed on the surface of GQD-1.

The edge-functionalization of GQD-1 with 4-propynyloxybenzyl groups is outlined in Scheme 1. GQD-1 was treated with oxalyl chloride under reflux conditions for 3 days. The reaction mixture was then subjected to an imidation reaction with benzylamine **4** at  $100^\circ\text{C}$  for 3 days. Subsequent chromatographic purification of the mixture on silica gel afforded GQD-2 as a brown powder. The introduction of the benzylamino group was confirmed by  $^1\text{H}$  NMR and IR spectroscopy (Figure 1a). The IR absorption spectrum<sup>[13]</sup> of GQD-1 showed broad absorption bands corresponding to hydrogen-bonded O–H groups ( $3700$ – $2300$   $\text{cm}^{-1}$ ). These bands were absent in the GQD-2 spectrum, and new bands were observed at  $3286$  and  $2119$   $\text{cm}^{-1}$ , attributable to  $\equiv\text{C}-\text{H}$  and  $-\text{C}\equiv\text{C}-$  absorptions, respectively, thus suggesting that most of the carboxylic acid groups at the GQD periphery had reacted with benzylamine **4**.

Armchair and zigzag arrangements are typical GQD edge structures (Figure 1b). To determine the edge structures of GQD-2, model compounds **M1**, **M2**, and **M3** were synthesized. The five-membered cyclic imide **M1** is formed only with the armchair arrangement in the region corresponding to the peripheral carbon atoms of GQD-2, whereas the zigzag arrangement is observed with the six-membered cyclic imide **M2**. Carboxylic acid **M3** is a possible product when the imidation reaction is not completed. Their IR spectra are presented in Figure 1a. **M3** generated sharp bands at  $3360$ ,

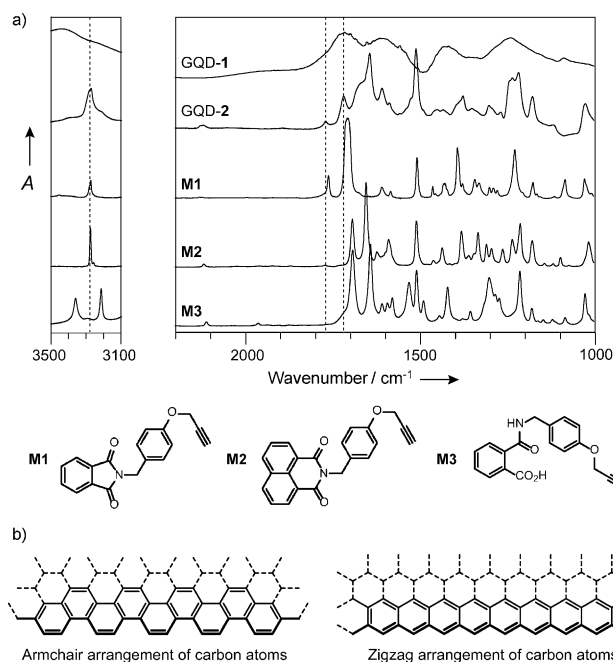


**Figure 1.** a) IR absorption spectra of GQD-1, GQD-2, **M1**, **M2**, and **M3**. b) Characteristic edge structures of graphene.

$3214$ ,  $1695$ , and  $1643$   $\text{cm}^{-1}$ , which are attributable to N–H,  $\equiv\text{C}-\text{H}$ , and two C=O groups, respectively. In the IR spectrum of GQD-2, the N–H absorption band was absent, while the  $\equiv\text{C}-\text{H}$  and C=O absorptions were shifted. Therefore, the presence of a 2-carbamoylbenzoic acid structure was not detected. The two possible cyclic imide structures represented by **M1** and **M2** displayed characteristic differences in their C=O absorptions. The weak and strong carbonyl bands of **M1** at  $1771$  and  $1717$   $\text{cm}^{-1}$  are characteristic of five-membered cyclic imides, whereas those of **M2** appeared at  $1695$  and  $1656$   $\text{cm}^{-1}$ .<sup>[14]</sup> GQD-2 exhibited weak and strong carbonyl

bands at 1765 and 1712  $\text{cm}^{-1}$ , corresponding to those of **M1**, thus indicating that the periphery of GQD-2 was principally functionalized with the phthalimide structure. Therefore, the peripheral carbon atoms of GQD-2 most likely adopt the armchair arrangement.

GQD-2 was soluble in the common organic solvents ethyl acetate, acetone, 1,2-dichloroethane, dichloromethane, tetrahydrofuran, and acetonitrile. The evident lipophilicity of GQD-2 is a result of the edge-functionalization of GQD-1 with 4-propynyloxybenzyl groups. Solutions of GQD-2 in these solvents were stable; no precipitation was observed when the solutions were left standing for more than a week. In general, graphene sheets often precipitate through self-aggregation. The high solution stability of GQD-2 suggests that the 4-propynyloxybenzyl moieties likely provide steric protection for the  $\text{sp}^2$  carbon surface, thereby preventing self-aggregation driven by  $\pi$ - $\pi$  stacking interactions.

Graphene quantum dots have aromatic surfaces that are large, flat, and flexible. Under certain conditions, these large surfaces are bent, folded, and twisted. Such structural distortions are expected to modulate the electronic properties of GQDs. The introduction of bulky substituents at the periphery of GQDs should generate a steric requirement for the expansion of the aromatic surface so that effective conjugation is extended. Therefore, we introduced dendritic wedges at the periphery of GQD-2. Dendrons **5a-c**, which possess an azide group, were incorporated onto GQD-2 through copper-catalyzed Huisgen cycloaddition (Scheme 1).<sup>[9a,c,15]</sup> The reaction of GQD-2 with **5a-c** was monitored by  $^1\text{H}$  NMR and IR spectroscopy. Figure 2 displays partial IR

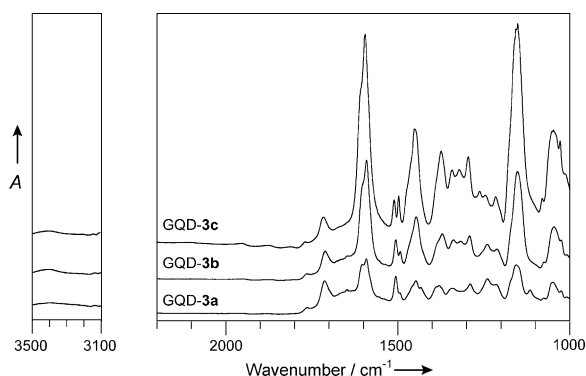


**Figure 2.** IR absorption spectra of GQD-3a-c.

absorption spectra for GQD-3a-c. Complete conversion of the triple bonds to triazole rings was evidenced by the disappearance of the  $\equiv\text{C-H}$  absorption band. GQD-2 smoothly reacted with **5a** over 48 h to give GQD-3a, whereas the reactions with **5b** and **5c** required more than 120 h, thus implying that the dendrons might generate severe steric congestion at the periphery of GQD-2 to reduce the reactivity of **5b** and **5c**. The incorporation of the dendritic wedges was confirmed by IR spectroscopy. Intense aromatic C-C absorptions of GQD-3a-c were located at approximately 1600  $\text{cm}^{-1}$ . The ratios of the aromatic C-C absorptions in proportion to the C=O absorptions increased along the series of GQD-3a,

**3b**, and **3c**, thus suggesting that the dendritic wedges were successfully incorporated at the GQD peripheries. The introduction of the dendritic wedges greatly improved the solubility of GQD-3a-c, which were even more soluble in ethyl acetate, acetone, 1,2-dichloroethane, dichloromethane, tetrahydrofuran, benzene, and chlorobenzene.

Atomic force microscopy (AFM) measurements of the GQDs provided detailed information about their sizes and dimensions. The statistical size distribution of  $(20 \pm 1)$  nm for GQD-2 indicates that oxidative cutting was effective in producing GQDs with a uniform size. It was estimated from TG/TGA analysis that approximately 60–70 4-propynyloxybenzylamine groups had been introduced at the GQD periphery. The incorporated dendritic wedges were directly visualized by AFM measurements. The AFM images of GQD-2 show trapezoidal morphologies with a height of 0.40 nm, approximately the size of an aromatic ring edge, although many agglomerated morphologies were observed (Figure 3a, c, d). The GQDs featuring dendritic wedges gave rise to unique morphologies; GQD-3b displayed a trapezoidal shape surrounded by higher walls (Figure 3b, e, f). The cross section revealed a center height of 0.48 nm, which is consistent with the thickness of a single-layered GQD, as well as two peaks heights of 0.64 nm, which confirmed that the dendritic wedges are successfully incorporated around the edges of the GQDs. GQD-3b was observed to be chiefly single-layered with a uniform diameter of  $(21 \pm 2)$  nm, thus

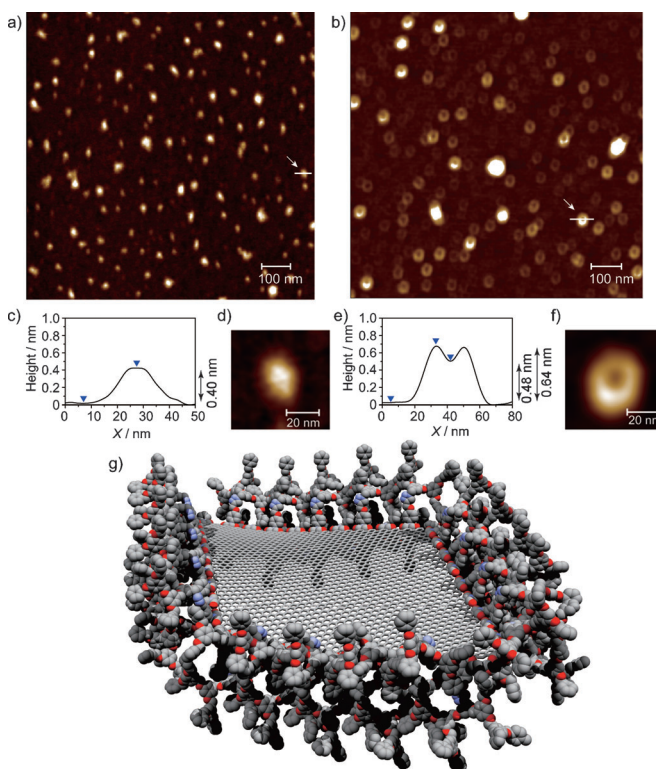


**Figure 3.** AFM images (topography) of a) GQD-2 ( $0.9 \mu\text{m} \times 0.9 \mu\text{m}$ ) and b) GQD-3b ( $0.9 \mu\text{m} \times 0.9 \mu\text{m}$ ) on mica disks. c, f) Height profiles of the cross sections of the white lines in (a) and (b), and magnified images of (d) GQD-2 and (f) GQD-3b. g) Calculated structure of GQD-3c.

strongly suggesting that the introduced dendritic wedges hamper its agglomeration in solution.

To visualize the plausible structure of edge-functionalized GQDs, molecular mechanics calculations were carried out with MacroModel V.9.1 using the OPLS2005 force field.<sup>[16]</sup> The resultant structure of a GQD with third generation dendron wedges is illustrated in Figure 3g. The dendritic wedges provide significant steric congestion that interferes with self-aggregation through  $\pi$ - $\pi$  stacking interactions. Bending, twisting, and folding of the GQD surface are most likely prevented, thus implying that effective aromatic conjugation can be extended as a result of steric effects. The optoelectronic properties of the GQDs should be responsive to the structures of the wedges at the periphery.

The UV/Vis absorption bands of GQD-2 and GQD-3a-c in dichloromethane appeared within the visible region (Figure 4a-d). The incorporation of dendritic wedges onto GQDs likely has a limited influence on the ground-state electronic structures, but the emission properties of the GQDs are quite noteworthy. Photoluminescence studies with GQD-2 and GQD-3a-c revealed that the emission maxima depended on the excitation wavelengths.<sup>[17]</sup> Upon excitation at 360 nm, GQD-2 exhibited an emission maximum at 411 nm, while the emission maxima of GQD-3a, 3b, and 3c were red-shifted to

546, 546, and 539 nm, respectively. The red-shifts of the emission maxima for GQD-3a-c were observed even upon excitation at wavelengths ranging from 360 to 480 nm. The absolute photoluminescence quantum yields of GQD-2 and GQD-3a-c in dichloromethane with excitation wavelength at 360 nm were approximately 1–2% and did not change at other excitation wavelengths. These observations imply that the excited states of GQD-3a-c are more stable than those of GQD-2. Although the precise mechanism of excited-state stabilization through the incorporation of dendritic wedges remains uncertain, the peripheral dendritic wedges of GQD-3a-c create significant steric interactions that restrict stacking, twisting, bending, and folding of the GQD surface. As a result, the effective conjugation of the aromatic surface of GQD-3a-c could be extended through steric effects and may result in the observed excited state stabilization.

The emission behaviors correspond to the optical images. Commission Internationale de l'Éclairage (CIE) 1931 chromaticity diagrams were employed to characterize the emission profiles of GQD-2 and GQD-3a-c. The CIE 1931 chromaticity coordinates for GQD-2 and GQD-3a-c when excited at 360 nm and for GQD-2 when excited at 380 nm were calculated, and a series of digital photographs of the corresponding samples in dichloromethane solutions under 360 and 380 nm light are presented (Figure 4e), along with the chromaticity coordinates in the CIE 1931 diagram (Figure 4f). GQD-3a-c exhibited white-light emission, an uncommon feature, upon excitation at 360 nm, while GQD-2 displayed bluish-white emission; however, excitation at 380 nm gave rise to white emission. The CIE 1931 chromaticity coordinates changed with an increase in the sizes of the dendritic wedges [e.g., GQD-2 ( $x=0.223$ ,  $y=0.214$ )→GQD-3c ( $x=0.324$ ,  $y=0.383$ )], thus indicating that the photoluminescence behavior of GQD-2 is tunable through introducing organic functional groups at the periphery of GQD-2.

In conclusion, we synthesized white-light-emitting edge-functionalized graphene quantum dots GQD-2 and GQD-3a-c through the reaction of edge-oxidized GQDs (GQD-1) with 4-propynyloxybenzylamine (4). <sup>13</sup>C NMR spectroscopy revealed that most regions of the sp<sup>2</sup> surfaces of GQD-1 were not oxidized. The lipophilicity of GQD-2 permits a range of chemical modifications in organic solvents for the development of optoelectronically functionalized carbon-based materials. Indeed, the optical properties of GQD-2 were tuned by functionalizing the edges with dendritic wedges, with the resulting GQDs demonstrating white-light emission. Because these lipophilic GQDs are chemically accessible, they hold promise for application in carbon-based materials that may become a source of unique optoelectronic devices.

Received: December 28, 2013

Published online: ■■■■■, ■■■■■

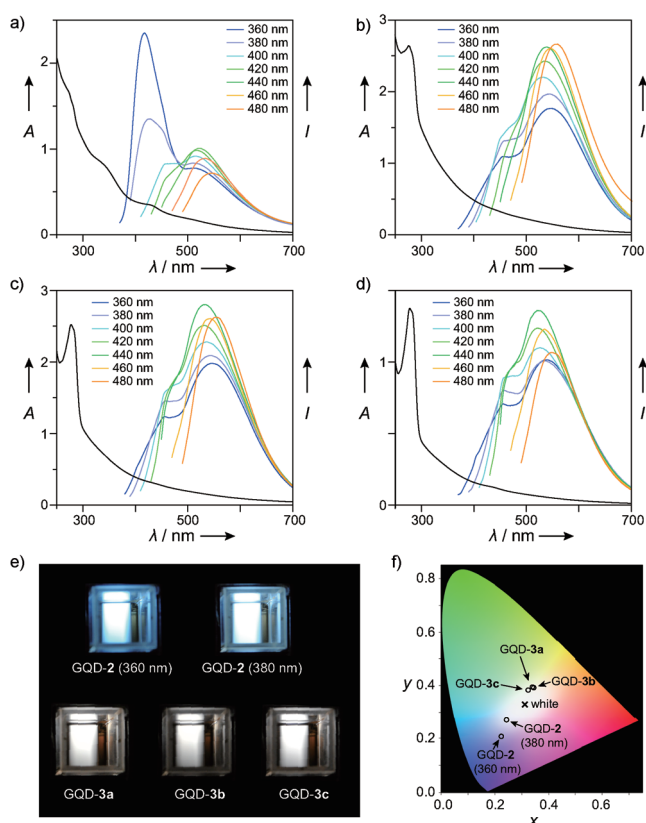


**Figure 4.** UV/Vis absorption and fluorescence spectra of a) GQD-2, b) GQD-3a, c) GQD-3b, and d) GQD-3c in CH<sub>2</sub>Cl<sub>2</sub>. e) Optical images of GQD-2 (360 and 380 nm), GQD-3a (360 nm), GQD-3b (360 nm), and GQD-3c (360 nm). f) The CIE 1931 chromaticity diagram of GQD-2 at 360 nm ( $x=0.223$ ,  $y=0.214$ ), GQD-2 at 380 nm ( $x=0.240$ ,  $y=0.265$ ), GQD-3a ( $x=0.336$ ,  $y=0.394$ ), GQD-3b ( $x=0.340$ ,  $y=0.392$ ), and GQD-3c ( $x=0.324$ ,  $y=0.383$ ).

**Keywords:** graphene · nanostructures · nanotechnology · quantum dots · white-light emission

[1] H. W. Kroto, J. R. Heath, S. C. O'Brien, R. F. Curl, R. E. Smalley, *Nature* **1985**, *318*, 162–163.

- [2] S. Iijima, *Nature* **1991**, *354*, 56–58.
- [3] a) V. Sgobba, D. M. Guldi, *Chem. Soc. Rev.* **2009**, *38*, 165–184; b) B. C. Thompson, J. M. J. Fréchet, *Angew. Chem.* **2008**, *120*, 62–82; *Angew. Chem. Int. Ed.* **2008**, *47*, 58–77; c) K. Holczer, O. Klein, S.-M. Huang, R. B. Kaner, K.-J. Fu, R. L. Whetten, F. Diederich, *Science* **1991**, *252*, 1154–1157; d) A. F. Hebard, M. J. Rosseinsky, R. C. Haddon, D. W. Murphy, S. H. Glarum, T. T. M. Palstra, A. P. Ramirez, A. R. Kortan, *Nature* **1991**, *350*, 600–601.
- [4] K. S. Novoselov, A. K. Geim, S. V. Morozov, D. Jiang, Y. Zhang, S. V. Dubonos, I. V. Grigorieva, A. A. Firsov, *Science* **2004**, *306*, 666–669.
- [5] a) Y. Zhang, L. Zhang, C. Zhou, *Acc. Chem. Res.* **2013**, *46*, 2329–2339; b) J. K. Wassei, R. B. Kaner, *Acc. Chem. Res.* **2013**, *46*, 2244–2253; c) C. Chung, Y.-K. Kim, D. Shin, S.-R. Ryoo, B. H. Hong, D.-H. Min, *Acc. Chem. Res.* **2013**, *46*, 2211–2224; d) D. Bitounis, H. Ali-Boucetta, B. H. Hong, D.-H. Min, K. Kostarelos, *Adv. Mater.* **2013**, *25*, 2258–2268; e) H. Shen, L. Zhang, M. Liu, Z. Zhang, *Theranostics* **2012**, *2*, 283–294; f) J. Liu, J. Tang, J. J. Gooding, *J. Mater. Chem.* **2012**, *22*, 12435–12452; g) I. V. Lightcap, P. V. Kamat, *Acc. Chem. Res.* **2013**, *46*, 2235–2243; h) V. Georgakilas, M. Otyepka, A. B. Bourlino, V. Chandra, N. Kim, K. C. Kemp, P. Hobza, R. Zboril, K. S. Kim, *Chem. Rev.* **2012**, *112*, 6156–6214; i) D. Chen, H. Feng, J. Li, *Chem. Rev.* **2012**, *112*, 6027–6053; j) M. J. Allen, V. C. Tung, R. B. Kaner, *Chem. Rev.* **2010**, *110*, 132–145; k) C. N. R. Rao, A. K. Sood, K. S. Subrahmanyam, A. Govindaraj, *Angew. Chem.* **2009**, *121*, 7890–7916; *Angew. Chem. Int. Ed.* **2009**, *48*, 7752–7777; l) J. Wu, W. Pisula, K. Müllen, *Chem. Rev.* **2007**, *107*, 718–747.
- [6] L. A. Ponomarenko, F. Schedin, M. I. Katsnelson, R. Yang, E. W. Hill, K. S. Novoselov, A. K. Geim, *Science* **2008**, *320*, 356–358.
- [7] a) X. T. Zheng, A. Than, A. Ananthanaraya, D.-H. Kim, P. Chen, *ACS Nano* **2013**, *7*, 6278–6286; b) J. K. Kim, M. J. Park, S. J. Kim, D. H. Wang, S. P. Cho, S. Bae, J. H. Park, B. H. Hong, *ACS Nano* **2013**, *7*, 7207–7212; c) M. Zhang, L. Bai, W. Shang, W. Xie, H. Ma, Y. Fu, D. Fang, H. Sun, L. Fan, M. Han, C. Liu, S. Yang, *J. Mater. Chem.* **2012**, *22*, 7461–7467; d) H. Tetsuka, R. Asahi, A. Nagoya, K. Okamoto, I. Tajima, R. Ohta, A. Okamoto, *Adv. Mater.* **2012**, *24*, 5333–5338; e) S. Zhu, J. Zhang, C. Qiao, S. Tang, Y. Li, W. Yuan, B. Li, L. Tian, F. Liu, R. Hu, H. Gao, H. Wei, H. Zhang, H. Sun, B. Yang, *Chem. Commun.* **2011**, *47*, 6858–6860; f) V. Gupta, N. Chaudhary, R. Srivastava, G. D. Sharma, R. Bhardwaj, S. Chand, *J. Am. Chem. Soc.* **2011**, *133*, 9960–9963; g) X. Yan, X. Cui, B. Li, L.-S. Li, *Nano Lett.* **2010**, *10*, 1869–1873.
- [8] W. S. Hummers, R. E. Offeman, *J. Am. Chem. Soc.* **1958**, *80*, 1339.
- [9] a) H. C. Kolb, M. G. Finn, K. B. Sharpless, *Angew. Chem.* **2001**, *113*, 2056–2075; *Angew. Chem. Int. Ed.* **2001**, *40*, 2004–2021; b) C. Hawker, J. M. J. Fréchet, *J. Chem. Soc. Chem. Commun.* **1990**, 1010–1013; c) R. Huisgen, *Pure Appl. Chem.* **1989**, *61*, 613–628.
- [10] J. Peng, W. Gao, B. K. Gupta, Z. Liu, R. Romero-Aburto, L. Ge, L. Song, L. B. Alemany, X. Zhan, G. Gao, S. A. Vithayathil, B. A. Kaiparettu, A. A. Marti, T. Hayashi, J.-J. Zhu, P. M. Ajayan, *Nano Lett.* **2012**, *12*, 844–849.
- [11] J. I. Paredes, S. Villar-Rodil, A. Martínez-Alonso, J. M. D. Tascón, *Langmuir* **2008**, *24*, 10560–10564.
- [12] W. Cai, R. D. Piner, F. J. Stadermann, S. Park, M. A. Shaibat, Y. Ishii, D. Yang, A. Velamakanni, S. J. An, M. Stoller, J. An, D. Chen, R. S. Ruoff, *Science* **2008**, *321*, 1815–1817.
- [13] A broadening of the spectrum might be due to aggregation of GQD-1 driven by hydrogen-bonding interactions.
- [14] a) D. Smith, P. J. Taylor, *J. Chem. Soc. Perkin Trans. 2* **1979**, 1376–1386; b) T. Matsuo, *Bull. Chem. Soc. Jpn.* **1964**, *37*, 1844–1848.
- [15] S. Lal, S. Díez-González, *J. Org. Chem.* **2011**, *76*, 2367–2373.
- [16] F. Mohamadi, N. G. J. Richards, W. C. Guida, R. Liskamp, M. Lipton, C. Caufield, G. Chang, T. Hendrickson, W. C. Still, *J. Comput. Chem.* **1990**, *11*, 440–467.
- [17] a) D. B. Shinde, V. K. Pillai, *Chem. Eur. J.* **2012**, *18*, 12522–12528; b) Y. Li, Y. Zhao, H. Cheng, Y. Hu, G. Shi, L. Dai, L. Qu, *J. Am. Chem. Soc.* **2012**, *134*, 15–18; c) J. Shen, Y. Zhu, C. Chen, X. Yang, C. Li, *Chem. Commun.* **2011**, *47*, 2580–2582.

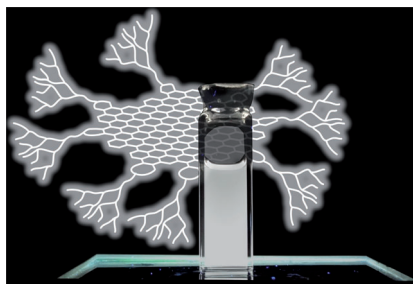
## Communications



### Graphene Quantum Dots

R. Sekiya, Y. Uemura, H. Murakami,  
T. Haino\* ————— ■■■■-■■■■

White-Light-Emitting Edge-  
Functionalized Graphene Quantum Dots



**In the dotlight:** Graphene quantum dots (GQDs) functionalized with bulky Fréchet's dendritic wedges at the GQD periphery were synthesized. The single-layered, size-regulated structures of the dendronized GQDs were revealed by atomic force microscopy. The edge-functionalization of the GQDs led to white-light emission, which is an uncommon feature.